

# A chromospheric conundrum?

Philip Judge and Michael Knölker

*High Altitude Observatory, National Center for Atmospheric Research<sup>1</sup>, P.O. Box 3000,  
Boulder CO 80307-3000, USA*

Wolfgang Schmidt and Oskar Steiner

*Kiepenheuer-Institut für Sonnenphysik, Schöneckstr. 6, D-79104 Freiburg, Germany)*

## ABSTRACT

We examine spectra of the Ca II H line, obtained under good seeing conditions with the VTT Echelle Spectrograph in June of 2007, and higher resolution data of the Ca II 8542 Å line from Fabry-Pérot instruments. The VTT targets were areas near disk center which included quiet Sun and some dispersed plage. The infrared data included quiet Sun and plage associated with small pores. Bright chromospheric network emission patches expand little with wavelength from line wing to line center, i.e. with increasing line opacity and height. We argue that this simple observation has implications for the force and energy balance of the chromosphere, since bright chromospheric network emission is traditionally associated with enhanced local mechanical heating which increases temperatures and pressures. Simple physical considerations then suggest that the network chromosphere may not be able to reach horizontal force balance with its surroundings, yet the network is a long-lived structure. We speculate on possible reasons for the observed behavior. By drawing attention to a potential conundrum, we hope to contribute to a better understanding of a long-standing unsolved problem: the heating of the chromospheric network.

*Subject headings:* Sun: atmosphere - Sun: chromosphere - Sun: surface magnetic fields

## 1. Introduction

Over a century ago, Hale and Ellerman (1904) obtained the first spectroheliograms of the disk chromosphere. Their work was the first to reveal the bright “chromospheric network” pattern, with scales of around 30Mm, at various wavelengths in the Ca II *H* and *K*

lines, and in  $H\beta$ . It is now known that the “Ca II network” overlies photospheric magnetic field concentrations clustered in supergranule downflow lanes (Simon and Leighton 1963; Simon and Leighton 1964; Skumanich *et al.* 1975; Schrijver *et al.* 1989).

The Sun’s network chromosphere emits variable UV radiation and sets the lower boundary conditions for the bulk of the overlying corona. It therefore determines and/or mediates the Sun’s radiative and particulate influence on the upper atmospheres of the earth and planets. Its importance in this regard stands in contrast to our basic understanding of it. While our knowledge of the dominant physical processes in the chromosphere is growing, the network component of the chromosphere shows behavior which particularly continues to challenge us (see, e.g. de Pontieu *et al.* 2007). There are both observational and theoretical reasons for this state of affairs. The chromosphere has a pressure scale height of  $\sim 125$  km, which subtends  $0''.18$  at the earth, and which is close to the resolution of modern chromospheric observations. It is also structured by magnetic fields at scales down to the limits of the instruments used. Non-LTE radiation transport presents a major difficulty, and the chromosphere contains highly dynamic phenomena when observed on the smallest scales.

In this era of large numerical simulations and data of unprecedented angular resolution, we take a step back to point out a simple observational fact that, to us at least, came as a surprise, and discuss its implications for our current understanding of the basic physics of the chromosphere. Our approach is based upon observational data and simple physical considerations. While MHD models exist, we avoid drawing heavily on these calculations because there is no credible, unique model for the heating of the network chromosphere, a subject of central interest to the present work. Our discussion is reminiscent of an early debate concerning force balance in sunspots (Alfvén 1943; Cowling 1976; Maltby 1977; Giovanelli 1982).

## 2. Observations

### 2.1. Slit spectra of the Ca II H line

Rammacher *et al.* (2008) reported on data obtained near the Sun’s disk center with the Echelle Spectrograph (ESG) of the VTT on Tenerife in June 2007. We use a subset of these data for the Ca II H line which they call “large x-y” maps. The Sun’s surface center was imaged onto the ESG slit, and the spectrograph dispersed the  $\approx 170''$  long section of the Sun’s light onto a detector with pixels every  $0''.33$  along the slit and every  $4.5$  mÅ in the wavelength direction ( $R = \lambda/\Delta\lambda = 900,000$ ). Each detector image was read into 513 spatial pixels by 976 wavelength pixels (spanning  $4.4$  Å). The slit was rastered across

the solar surface at angles tilted slightly in the S-N direction, with steps of  $0''.5$ , yielding a field of view of  $170'' \times 120''$ . The data were flat-field and dark corrected using standard techniques. Table 1 lists the circumstances of these observations. Data for 13 June 2007 were of a mostly unipolar part of a small, decaying active region, the other data were of quieter regions containing mixed polarities. The seeing, measured by  $r_0$ , was classified as good. The adaptive optics system at the VTT provided good image quality and excellent pointing stability during the raster scans. The measured angular resolution, judged from spatial power spectra, is typically 1.25 times the Nyquist sampling limits of  $0''.66$  and  $1''$ , varying between 1 and 2 times these limits depending on instantaneous seeing conditions.

Figure 1 places the ESG scan for 13 June 2007 into the context of a SOLIS synoptic magnetogram scan obtained from 14:21 UT to 14:33 UT at  $6302 \text{ \AA}$ . In the figure the SOLIS data have been rotated back to the time of the ESG observations, 10:54 UT. The corresponding line center data from the ESG are shown in Figure 2. In the latter figure, chromospheric fibrils with structures down to the sampling-limited resolutions are visible, confirming that the seeing was indeed good and the instrument stable. The boxed regions in the figure outline concentrations of bright Ca II emission, overlying regions of predominantly positive magnetic flux (Figure 1) associated with chromospheric network emission at various intensity levels. The size of these boxes was chosen as  $30'' \times 30''$ , sufficiently large to examine the widths of the bright Ca II network emission, but slightly smaller than the scale of supergranulation itself.

Figure 3 shows images at selected wavelengths across the Ca II H line for the data obtained on 13 June 2007. The images were constructed at each wavelength listed for each sub-frame of Figure 2 by summing over five wavelength bins (a  $22.5 \text{ m\AA}$  bandpass, corresponding to a resolution of 180,000). Images on the short wavelength side of the line are qualitatively similar. In all cases, *the bright chromospheric network emission does not expand much as the center of the Ca II H line profile is approached*. The data at 1000 and 399 mÅ show the reverse granulation associated with the upper photosphere, and bright network emission. Closer to line center, the bright emission changes character to fibril-like structures familiar in the H $\alpha$  literature, but *the emission expands very slightly, if at all*. Instead, there is an apparent smearing or “filling-in” of the granular structure visible at wavelengths farther from line center.

To quantify this observation, Figure 4 shows characteristic scales in the images computed from the network features centered in the boxes shown in Figure 3 and for other boxed regions (not shown) for the other two datasets. Characteristic widths  $w_N$  (FWHM) of the network features were computed as follows. First we subtracted the intensity at the lowest 3% of the intensity distribution for each sub-image, to permit us to measure the widths of the emission

peaks above typical background levels. (The choice of 3% is not critical). To remove edge effects edges of each such sub-image were apodized using a cosine bell function. The areas of pixels  $A_{50}$  which exceed 50% of the peak intensity were computed, and the widths were determined from  $\pi w_N^2/4 = A_{50}$ . The widths are therefore a characteristic FWHM of the brightest features at the centers of the sub-images. The results are plotted as a function of wavelength for each sub-image (Figure 4).

In all three datasets a trend emerges: widths  $w_N$  of line core images are similar to or only marginally larger than those of the line wings. In scan 2 obtained on 13th June 2007, of plage in a small active region, the median data for the line cores have scales of 9-10'', just 20% larger than measured at wing wavelengths. In the other two datasets, quieter regions, the cores widths are  $\lesssim$  40% larger than the widths measured in the wings.

We conclude that Ca II H line core images of bright network elements, as seen at the  $\lesssim$  1'' resolution of our VTT data, have geometric scales only marginally ( $\leq$  40%) larger than those for the underlying wing images. There is a hint that at wavelengths between  $H_3$  and  $H_{2V}$ , the widths of structures are narrower than the  $H_2$  peaks on the red and blue side of the line.

## 2.2. Data of higher angular resolution

The highest resolution (0'.1) images of photospheric magnetic flux concentrations reveal structure in the network down to the diffraction limit (e.g. Berger *et al.* 2004). The question then arises as to the interpretation of data with the  $\sim$  1'' resolution data studied above. To study network expansion with height, a spectral resolution of  $R \gtrsim$  50,000 is needed to resolve chromospheric line profiles (Reardon *et al.* 2009). Thus, well-studied but relatively broad band Ca II H or K line images (e.g. from the Dutch Open telescope with  $R \sim$  3000, the Swedish Solar telescope with  $R \lesssim$  3500, the Hinode spacecraft  $R \sim$  1000) cannot address this problem directly. The present generation of Fabry-Perot imaging spectroscopic instruments with  $R \gtrsim$  100,000 and chromospheric capabilities, including IBIS (Cavallini 2006), CRISP (Scharmer *et al.* 2008), and GFPI (Bello González and Kneer 2008), can in principle shed light on the problem addressed here. In particular, with adaptive optics and image reconstruction techniques, such instruments can achieve far higher angular resolution.

Surprisingly few published studies are of direct relevance to the problem at hand. Leenaarts *et al.* (2009) compare CRISP data for the 8542 Å line of Ca II with MHD simulations. The bright emission over flux concentrations is confined to subarcsecond structures in their figure 3 showing both observations and calculations. Care must be taken in drawing

quantitative conclusions from their work because color tables are different between the panels in their figure. Furthermore, the relationship of these observations and models to conditions in “standard” models of the network chromosphere, discussed below, is not clear.

Figure 1 (panel a) and Figure 2 (panel e) of Vecchio *et al.* (2007) show wing and core intensity images of the 8542 Å line, from IBIS observations of a mixed polarity region of quiet Sun. Expansion of the bright network appears to be a factor of several from wing to core. Yet, in their data, there exist bright knots of Ca II emission at core wavelengths, within the expanded network emission, on sub-arcsecond scales. Again individual color tables are different for different panels. To quantify the expansion of the network seen in the 8542 Å line, we have re-examined the sharpest images ( $\sim 0''.5$  resolution) of an IBIS dataset by Judge *et al.* (2010), of small pores and active network. Qualitatively these images appear similar to those of the cited work of Vecchio and others. The net intensities of Ca II wing and core data are shown here in Figure 5, where the intensity of the lowest 5% level in the intensity distribution has been subtracted to remove the darkest non-magnetic features. Over-plotted as contours are 50% contours of the wing and core net intensity images (solid and dashed lines respectively). The dotted lines are 70% core contours, shown because these contain a similar relative area to the wing 50% contours. The 50% intensity contours of the core are far broader than those of the wing data. However, the network contains much structure at the 70% core intensity level which lies within just a couple of arcseconds of the underlying bright wing emission.

These higher angular resolution data indicate that the brightest knots of chromospheric network emission are confined to within  $\sim 2''$  of the underlying photospheric emission, but that they are often displaced significantly from the underlying bright photospheric magnetic features. Further expansion of the chromospheric magnetic field into the network cell interiors is seen only as dimmer features associated with fibrils expanding into the surrounding area.

### 3. Discussion

While significant small-scale dynamics can be observed on timescales down to seconds (e.g. de Pontieu *et al.* 2007), the network pattern’s lifetime is on the order of a day. But sound waves cross a 30Mm structure in about an hour, a 3Mm wide patch of magnetic network boundary in a few minutes. The overall network structure should therefore be close to (magneto-) static equilibrium, and we proceed assuming this to be the case.

### 3.1. A dilemma?

Characteristic scales of Ca II images of bright network elements are similar in the line core to those in the wings, yet optical depths in the wings of the lines beyond  $1\text{\AA}$  from line center are several orders of magnitude smaller than core optical depths. One dimensional atmospheric models (e.g. Vernazza *et al.* 1981, henceforth “VAL”) place the formation of the wings and core of the H line near 0.4 and 1.9 Mm above the continuum photosphere respectively, where the corresponding gas pressures are  $\sim 5 \times 10^3$  and  $\sim 4 \times 10^{-1}$  dyn cm $^{-2}$ . To satisfy force balance, the magnetic fields must expand horizontally with height through the chromosphere. In the Fabry-Pérot images, this expansion is seen as relatively dark fibrils extending into the internetwork regions. *But why, then, does the brightest Ca II emission expand far less than the magnetic field with height in the chromospheric network?* To address this question, we first review conditions in the photosphere and corona-chromosphere transition region, afterwards discussing the chromosphere in this context. This lack of observed expansion we call “confinement”.

### 3.2. Why the photospheric network is bright and confined

Lites *et al.* (2004) presented perhaps the clearest observations of the bright network, otherwise known as “faculae” when seen in photospheric features. These observations are compatible with a well known physical picture (as reviewed by Steiner 2007). Photospheric magnetic fields are forced by convective flows to collect in downflow vertices, where they exert significant pressure. Time-averaged force balance requires that plasma pressure inside the magnetic concentration be lower than outside, leading to less material, less opacity there. The concentrations therefore allow radiation from the “hot walls” of the atmosphere in which they are embedded to penetrate into them and out of the atmosphere. This is why faculae are bright.

### 3.3. Why the transition region network is bright and confined

The network seen in overlying transition region emission is also bright, but the network pattern disappears near coronal temperatures of  $10^6\text{K}$  (Tousey 1971; Reeves 1976). The physical reasons that this network is bright and confined are different from the photospheric case. At least two interpretations have been proposed in the literature.

Gabriel (1976) considered a magnetostatic network model embedded in an atmosphere with a magnetic and a non-magnetic component. The magnetic field, assumed unipolar, was

confined to network boundaries at the photosphere and was space-filling high in the corona, producing the characteristic “wine-glass” shape of field lines. Gabriel solved for a magnetic field that is potential everywhere inside the wine glass, and zero outside it, except at the current-sheet boundary between the flux concentration and the network cell interior. (He had to solve for the location of the boundary by requiring pressure balance across this current sheet). He then obtained thermal structure by imposing a balance between the divergence of conductive flux down from the (uniform) corona and radiation losses. He showed that transition region emission is confined over a several Mm wide area over the stem of the wine glass. In this model, “confinement” of the emission over the network occurs because energy is ducted from the corona along field lines which are defined by the magnetic morphology, which in turn is defined by the boundary conditions at the photosphere, corona and the current sheet.

A second picture recognizes that such models, based on classical heat conduction, fail to account for the brightness of lines formed in the transition region below  $10^5\text{K}$ . Some have also argued that morphology of images of the network transition region are inconsistent with such models (Feldman 1983). Thus Dowdy *et al.* (1986) have proposed that network transition region is emitted from plasma confined to relatively cool magnetic loops (Antiochos and Noci 1986) which close within the network boundaries themselves to opposite magnetic polarities, and which do not reach coronal temperatures. This picture itself has theoretical and observational problems and remains a subject for debate (Cally and Robb 1991; Judge and Centeno 2008).

The nature of the spatial confinement of bright transition region emission is quite different in the two cases. The cool loop picture requires that the plasma pressures be lower than the magnetic pressures otherwise the loop structures would tend to expand- the confinement is due to forcing. But, within the transition region in Gabriel’s model, the plasma pressure is irrelevant, as the magnetic field is potential there- the confinement is caused by field-aligned conductive energy transport. Typical gas pressures within the transition region network are  $p \sim 0.3 \text{ dyne cm}^{-2}$  (e.g. Mariska 1992; Doschek *et al.* 1998), the corresponding magnetic pressure requires  $B \sim 10^1\text{G}$ . Yet Gabriel’s solution used  $B = 1\text{G}$ , and he would have obtained qualitatively the same type of confinement for a wide range of field strengths, it depending just on the boundary distributions of magnetic field at the photosphere, corona, and the current sheet location. But in the case where the plasma  $\beta = p/(B^2/8\pi)$  is  $\gg 1$ , any perturbation of the force balance by plasma pressure gradients and/or gravity will force the magnetic field to a non-force free state in which the magnetic field can be pushed around. Given the dynamic nature of the observed transition region (Mariska 1992) and the injection of mass from the chromosphere below (de Pontieu *et al.* 2007), it may be that Gabriel’s potential field calculation is a singular case which may not occur in reality. Taken together, it

seems that confinement both by field-aligned energy transport and by force balance ( $\beta \leq 1$ ) may be required to explain the observed properties of transition region plasmas.

### 3.4. Why the chromospheric network is bright

Traditionally, the chromosphere is believed to be bright because of mechanical heating (e.g. Osterbrock 1961). The required dissipated energy flux density, derived from the need to account for radiation losses computed from 1D semi-empirical models, is on the order of  $10^7 \text{ ergs cm}^{-2} \text{ s}^{-1}$  (Avrett 1981; Anderson and Athay 1989), some four orders of magnitude smaller than the photospheric radiative flux density. Such calculations remain the best way to estimate the energy requirements, since they cannot be derived from observations alone for varied reasons. Yet the calculations, based upon observations which do not resolve structure below granular scales, contain little of the physics of magnetic concentrations. The photospheric parts of these models are almost identical, containing no multi-dimensional transfer such as the hot wall effect requires. As a result, any hot wall radiation re-radiated by the chromosphere is entirely ascribed to mechanical heating. We return to this issue in section 3.7.1, But first we argue that a difficulty arises when trying to understand why an entirely mechanically heated chromospheric network is *confined*.

### 3.5. Why is the bright chromospheric network confined?

While credible physical models of the chromosphere outside of magnetic concentrations are available (Carlsson and Stein 1995, 1997), none is available for the magnetized regions. We must deal instead with the semi-empirical models of network that are available, such as from VAL, recognizing their limitations along the way.

Chromospheric heating results in larger temperatures, and gas pressures, at a given height. Semi-empirical models of bright chromospheric features, such as those over network boundaries, are always accompanied by higher gas pressures and energy densities. But this is precisely the place where magnetic pressures are also higher. Herein lies a possible problem. Taken at face value, in particular the run of gas pressures with height, the semi-empirical models cannot be in horizontal force balance, as the network boundary model would be expected to expand horizontally until pressure exerted by neighboring magnetic fields and/or the magnetic tension force can balance the excess total pressure!

This dilemma is resolved in part through explicit recognition of 2D effects and the fact that the height scales of such models are defined with respect to the radial  $5000 \text{ \AA}$



continuum optical depth unity surface ( $\tau_{5000} = 1$ ). The hydrostatic equation used in the models yields  $p$  as a function of height  $z$  only to within a constant integration factor. In 2D, horizontal force balance requires gas pressures within photospheric flux tubes to be smaller at each height than outside it. The opacity is reduced, and the  $\tau_{5000} = 1$  surface is thus shifted downwards (the “Wilson depression”). On this basis Solanki and Steiner (1990) and Solanki *et al.* (1991) built “1.5D” models of flux tubes, endowed with thermal conditions of hotter and brighter models, e.g. VAL model F, embedded in cooler models. The entire flux-tube atmosphere (not just the photosphere) was moved downwards by 200 to 500 km, to satisfy horizontal force balance within the photosphere, depending on the combination of thermal structure and field strength used. The authors examined models with field strengths between 1500 and 1630G. Higher up, these authors iterated the magnetostatic equation to equilibrium, keeping the thermal structure within the two components fixed, both being a function of height only. Above a certain height (the “flux merging” height), although the plasma by itself cannot reach horizontal force balance (see Figure 6), in the models of Solanki and colleagues the magnetic field bumps into its neighbors, thereby taking up the net horizontal pressure gradient. In these 1.5D models,  $\tau = 1$  surfaces of network chromospheric features are geometrically lower than those of the non-magnetic surroundings. The emission is effectively confined and our dilemma appears resolved, at least qualitatively.

However, consideration of the physics underlying these calculations leads us to conclude that the ability of such 1.5D models to achieve magnetostatic equilibrium is remarkable. Wilson depressions of the magnetized photosphere are determined by the force balance only at *photospheric* heights. But the variation of *chromospheric* plasma pressure with height is determined largely by the unknown process(es) of chromospheric heating which occur many scale heights above the photosphere. Further, thermal structures in these semi-empirical models are in large part based upon observations, with no explicit treatment of force balance except through the constraint of vertical (1D) hydrostatic equilibrium. There is in fact *no prior reason to expect that the physics of chromospheric heating will accommodate the conditions needed for 3D magnetostatic equilibrium there, simply by dropping the network atmosphere by the amount needed to bring the photosphere into horizontal pressure balance.* We raise additional concerns.

- $B = 1500\text{G}$  is near the high end of a broad distribution of observed photospheric network field strengths (Berger *et al.* 2004) and in MHD models (Schaffenberger *et al.* 2005; Wedemeyer-Böhm *et al.* 2007). Lower values of  $B$ , keeping other parameters constant, means larger values of  $\beta^*$  (the asterisk refers to the value of  $\beta$  measured within the flux concentration, at the geometric height of the non magnetic photosphere). For a pressure scale height  $h$ , and given a value of plasma  $\beta^* < 1$ , the depression  $\delta$  of the photosphere required to bring it to photospheric force balance is  $\delta \approx h \ln(1 + \beta^{*-1})$ .

Solanki *et al.* (1991) present calculations where  $0.02 \leq \beta^* \leq 0.3$ . The photospheric gas pressure is  $1.2 \times 10^5 \text{ dyn cm}^{-2}$ , so for  $B = 1500, 1000, 500\text{G}$  we find  $\beta^* = 0.34, 2.0, 11$ , and with  $h = 120 \text{ km}$ ,  $\delta = 166, 49, 10 \text{ km}$  respectively. Even when  $\delta \sim 166 \text{ km}$  the gas pressures alone in models F and P exceed those of model A at chromospheric heights above 1.2 Mm (Figure 6). When  $\delta < 50 \text{ km}$  essentially the entire chromospheric gas pressures of models P and F exceed those of model A.

- At the very edge of photospheric faculae, there is no neighboring flux tube to balance excess pressure, a situation yet more dramatic when the embedding atmosphere has no chromospheric temperature rise such as is the case in the dynamic models (Carlsson and Stein 1995). Fig. 2 of Solanki and Steiner (1990) implies that the gas pressure surpasses the outside pressure already at 800 km and 850 km for  $B=1300$  and 1500 G, respectively.

There appears to be no easy way to make horizontal forces balance across bright network boundaries in the chromosphere in such models. At the very least we must understand why the chromosphere produces the brightest emission only directly over the photospheric magnetic concentrations.

### 3.6. What is the chromospheric plasma $\beta$ in network boundaries?

In both the chromosphere and transition region, the plasma  $\beta$  is a critical parameter, since as in plasma devices, confinement by magnetic forces requires  $\beta < 1$ . We expect  $\beta$  to vary both along and between field lines through the chromosphere, as the flux tubes are in no sense “thin”. The atmospheric stratification is strong (scale heights  $h$  are  $\sim 120 \text{ km}$  in a chromosphere of thickness  $\sim 1500 \text{ km}$ ), so that we expect  $\beta$  generally to decline with height. Upper limits to  $\beta$  extending though the chromosphere can be estimated using simply the net magnetic flux density averaged over a supergranular cell, assuming it is homogeneous. In quiet regions the mean field strength will be typically zero but with fluctuations of a few tens of  $\text{Mx cm}^{-2}$ . In more active network and plages this will increase to  $\gtrsim 100 \text{ Mx cm}^{-2}$ , in sunspot umbrae (for comparison) it will be  $\gtrsim 2000 \text{ Mx cm}^{-2}$ . Applying these estimates to VAL’s model F, we expect  $\beta = 1$  in quiet, plage and umbral regions to occur below heights of 1.2, 0.65 and -0.05 Mm respectively.

Direct observational determinations of  $\beta$  are rare because magnetic measurements using chromospheric features is difficult. Most such work has been concerned with sunspots (Metcalf *et al.* 1995; Socas-Navarro 2005), but network fields were studied by Pietarila *et al.* (2007b,a). The latter were made in plages associated with a decaying active region. Pietarila *et al.*

(2007a) made inversions for a region of predominantly negative polarity with a net mean flux density of order  $50 \text{ Mx cm}^{-2}$ . (This value was estimated by eye from Figure 2 of Pietarila *et al.* 2007b.) The longitudinal component of the field strength could be determined only near  $\tau_{5000} = 0.1$  and  $10^{-5}$ . Using the range of values of field strengths from their fig. 12 (network element), and assuming thermal parameters from VAL’s model F, the plasma  $\beta$  values are probably between 5 and 100 (at 0.15 Mm height) and 0.1 (at 1.1 Mm). The  $\beta = 1$  level probably lies near 0.5 Mm.

In truly quiet regions no measurements exist, but likely values of the plasma  $\beta$  can also be examined using “realistic” simulations<sup>1</sup>. Schaffenberger *et al.* (2005, 2006) have made simulations of magnetconvection extending 1.4 Mm above the photosphere, for an average field of  $10 \text{ Mx cm}^{-2}$ . In this case, there is not enough flux for the granulation to gather up and form the most intense 1.5 kG photospheric flux tubes- their field strengths are  $\leq 1$  kG. The computed  $\beta = 1$  surface lies near 1.2 Mm above the photosphere, i.e. well within the chromosphere, yet in their calculations no explicit or significant chromospheric heating was included to enhance chromospheric temperatures and pressures. The existence of field strengths mostly at or below 1 kG in the photospheric network (Berger *et al.* 2004) implies that  $\beta \geq 1$  in the lower parts of the chromosphere (Hasan and van Ballegooijen 2008).

We conclude that the lower 0.5-1 Mm or so of the network chromosphere is probably in a high  $\beta$  regime, depending on local conditions.

### 3.7. Mechanisms for confining chromospheric network emission

#### 3.7.1. Radiative energy transport

It is almost universally believed that the chromosphere is bright because of non-radiative, or mechanical, heating. However, Uitenbroek (private communication, 2009) has pointed out that Ca II H emission reversals can occur when the photospheric “hot wall” radiation raises the source functions and brightness of the Ca II wavelengths which are normally considered chromospheric. Such bright emission from the chromosphere is indeed expected to be confined to within a volume where the hot wall radiation can influence the source functions, the “thermalization volume”. 2D or 3D radiative equilibrium calculations are needed not only

---

<sup>1</sup>We have deliberately avoided use of simulations for the interpretation of chromospheric brightness, because brightness depends exponentially on the temperature and the heating mechanism(s) are not known. Our use here is also questionable, but estimates of the plasma  $\beta$  from simulations are arguably more reliable, at least for the first few scale heights of the chromosphere.

to relax the constraint of LTE, but also to take proper care of energy transport in spectral lines. The treatments made so far including opacity distribution functions and multi-group methods (Steiner 1990; Skartlien 2000) all adopt the coherent scattering approximation, thereby artificially reducing the range of influence of energy transport in spectral lines. The thermalization lengths are too low, the lambda- and other operators for lines are spatially too narrow. It remains to be seen if a more physical treatment of lines leads to significant differences with these calculations. Interestingly, Bruls and Von der Lühe (2001) found only small intensity enhancements in the  $H_{2R}$  peak and  $H_{1R}$  minimum, from a 2-D hot wall nLTE calculation again using semi-empirical models, suggesting that this effect may be small. But no self-consistent radiative equilibrium model has yet been performed.

However, transport of hot wall radiation cannot fully resolve the present dilemma, because it cannot account for emission lines requiring electron temperatures in excess of the temperature of the hot walls, such as UV and EUV lines. Nor can it explain the properties of bright knots of chromospheric emission in the line cores in data such as those shown in Figure 5. Also, the opacity may simply be just too large to permit transport of much energy from the hot walls into the body of the chromosphere. Nevertheless we note that essentially all mechanical heating requirements of the chromosphere are based on 1D semi-empirical models which do not include hot wall radiation. These requirements may therefore have been uniformly over-estimated, and deserve attention.

### 3.7.2. *Stresses on network boundaries*

Network cell interiors are not static, field-free structures. The possibility arises then that work might be done on the supergranular network by the horizontal components of waves, flows and by magnetic stresses associated with the cell interior chromosphere. Outside of shock waves and the eye-catching type-II spicules (de Pontieu *et al.* 2007) which are insignificant components of the bulk chromosphere, being phenomena of the more tenuous upper chromosphere (Judge and Carlsson 2010), spectral line shifts and proper motions indicate sub-sonic motions. Thus flows and waves can make only small contributions to the work done on supergranule boundaries compared with thermal pressure gradients.

Magnetic fields in the cell interiors have received increasing attention in recent years (e.g., Lites *et al.* 2007). Such fields may perhaps provide additional stress at the network boundaries, but they would need to compete with the strong network boundary fields to contain the excess pressure implied above. There is no evidence that these fields are strong enough to maintain a force at the edges of network boundaries sufficient to contain significant plasma over-pressure, if present.

### 3.7.3. Pinch effect

Simple flux ribbons and untwisted flux tube-models have no degree of freedom which might allow enhanced plasma pressures when  $\beta \gtrsim 1$ . However, if the bright Ca II network emission is associated with strongly twisted magnetic fields, the twist can “pinch” the plasma in network boundaries, potentially enhancing the pressures where magnetic fields are strong. It seems unlikely that the large body of data supports this picture, given that much of the network appears to be associated with flux sheets in granular downflow lanes (e.g. Berger *et al.* 2004), but the consequences of such a picture are of potential interest.

Many theoretical twisted flux tube models have been made, beginning with Parker (1974, 1977). Parker studied the analytical properties of force-free tubes which have slowly varying radii  $r$  with distance along the tube  $z$ , i.e.  $\partial r/\partial z \ll 1$ . His essential finding is that the degree of twist increases with the tube’s radius, the field becoming entirely azimuthal when the radius exceeds a critical level. The increasing twist results from the conservation of magnetic flux and torque (equivalently, electric current) along the tube. As a consequence, expanding tubes suffer increasing twist which eventually overcomes the pressure gradient force. Parker invoked this “pinch” or “buckling” effect as a way to release magnetic free energy in the much larger scale context of emerging solar active regions. Non-linear numerical calculations were made, for example, by Steiner *et al.* (1986), confirming Parker’s picture. By examining conditions high in the atmosphere where flux tube merging has occurred, these authors derived an upper limit to the twist at the tube’s base,  $B_\phi/B_z < \sqrt{f}$ , where  $f$  is the area filling factor of the tube at its base. This limit was obtained in the low- $\beta$  limit when the tension force  $\sim B_\phi^2/4\pi r$  exceeds magnetic pressure gradients  $\frac{1}{8\pi} \frac{\partial B^2}{\partial r}$  within the tube. It is precisely near this limit that the pinch may therefore be expected to compress the plasma in a higher  $\beta$  regime. In the quiet Sun,  $f \lesssim 0.01$  or so, so that  $B_\phi$  can at most be 10% of  $B_z$  in the photosphere. Beyond this twist, the merged fields in the upper part of the tube become unstable to the pinch effect. The evolution after pinch onset is not known.

The plasma pressure differences in the VAL cell and boundary models A and F are on the order of the pressures themselves, so that the twist must be near this limiting case if it is to account for the inferred thermal properties. In this case then the field becomes predominantly azimuthal. When  $f = 0.01$ , this requires that the tube expands radially tenfold over the value at the base. For a flux tube with base radius of 0.1 Mm the chromospheric twisted tube radius would become 1Mm, a value not inconsistent with the observed widths of the supergranular network. The dynamic consequences of such a situation are speculated upon below.

A recent letter reports Mm-scale swirling chromospheric motions above network elements in coronal holes (Wedemeyer-Böhm and Rouppe van der Voort 2009), apparently

driven by random granular motions below. Such motions, visible in the relatively uncluttered magnetic field in coronal holes, are probably related to this scenario. It is notable that there is no obvious relationship of the observed chromospheric brightness to these swirling motions.

#### 3.7.4. *Steady-state dynamics vs. static equilibrium*

A different resolution of our dilemma may lie in the possibility that the system is never close to equilibrium, but appears so when seen with existing instruments. By analogy, one might consider a cloud pattern which appears stationary when seen from a large distance, but closer observation reveals a non-steady dynamic evolution of individual clouds.

The intensity of chromospheric features like Ca II H scales exponentially with temperature, so that positive fluctuations in space and/or time in  $T$  might produce emission sufficient to account for the observed cell/ boundary intensity differences, while maintaining approximately magnetostatic balance in horizontal planes. This kind of picture is valid, at least in part, in the cell interior regions (Carlsson and Stein 1995, 1997). Acoustic gravity waves there propagate upwards and shock near 1 Mm above the photosphere to produce occasional bright bursts of chromospheric emission on top of a weaker, unresolved background emission. The time-averaged emission in their computations of Ca II lines, where  $h\nu/kT \gg 1$ , arises from a plasma in which the average temperature is far lower than would be required to produce the emission in a static model. In this case the average pressure is also less than a static model would require. The difference between the network boundary and cell interior problems is that there is much observational support for the waves in the latter case, but our knowledge of the mechanism(s) of network boundary heating and dynamics is not at all clear (see, for example Lites *et al.* 1993; Judge 2006).

Suppose, as in the cell interior case, that energy is released in the network boundary chromosphere intermittently but on time scales less than the boundary wave crossing time of  $\tau_w \sim w/c_s \sim 5$  minutes. Here  $w \sim 3$  Mm is characteristic scale of the network boundary thickness,  $c_s$  is the sound speed, and we assume  $\beta \gtrsim 1$ . The time scale for reaching ionization equilibrium is  $\sim 40$  seconds, being determined by the long times needed for hydrogen to recombine. Energy released as heat can be stored as latent heat of ionization on time scales longer than this. The radiative relaxation time  $\tau_{rr}$  of chromospheric plasma is

$$\tau_{rr} \sim \frac{1}{\gamma - 1} \frac{nkT}{\Phi},$$

where  $\Phi$  is the radiative energy loss rate per unit volume. When perturbations occur faster than the ionization time scale we can use  $\gamma = 5/3$ , since no change of internal state occurs.

From figure 4 of Anderson and Athay (1989) we find  $\Phi \approx 300m \text{ erg cm}^{-3} \text{ sec}^{-1}$  for heights  $> 1\text{Mm}$  (column mass  $m < 10^{-3} \text{ g cm}^{-2}$ ). This value applies to average quiet Sun conditions- $\Phi$  for the hotter network will be larger. Hydrostatic equilibrium gives  $p = nkT = mg$ , with  $g$  the gravitational acceleration, and the radiative cooling time becomes

$$\tau_{rr} \lesssim \frac{3}{2} \frac{mg}{300m} \sim 140 \text{ sec},$$

which is independent of  $m$  and smaller than  $\tau_w$ . ( $\tau_{rr}$  increases rapidly in deeper layers owing to radiative transfer effects.) Thus, chromospheric plasma can in principle store energy as latent heat of ionization and radiate it faster than sound waves can communicate any overpressure to the network cell interiors. This state of affairs is precisely what is needed to sustain a bright non-equilibrium network chromosphere heated intermittently on time scales shorter than  $\tau_w$ , while at the same time avoiding a sustained large horizontal pressure imbalance between the network boundary and the cell interior.

This suggestion might have support observationally, as the network chromosphere is the site of significant small scale “activity”. Spicules originate from these regions (Beckers 1972). Time series spectral observations, including the chromospheric Ca II  $H$  line, obtained by Lites *et al.* (1993), show marked differences between network cell boundaries and interiors. Cell boundaries show variability on time scales of 5 minutes and longer, which appear to show features propagating slowly away from the peak of the network emission, with apparent speeds of a few km/s ( $\lesssim 1$  to 2 Mm in 5 minutes). These features repeat perhaps every 8-10 minutes. There is as yet no accepted physical model for this network behavior.

Recent MHD simulations extending from the convection zone to 1400 km above the photosphere also lend credibility to this possibility<sup>2</sup>. Schaffenberger *et al.* (2005); Wedemeyer-Böhm *et al.* (2007) have found that the magnetized part of the chromosphere behaves quite differently from the underlying photosphere, albeit for average magnetic flux densities near  $10 \text{ Mx cm}^{-2}$ , weaker perhaps than present in the data examined here. Nevertheless, while the calculations support the general idea of quasi-static “canopy” fields, the magneto-fluid over the photospheric flux concentrations is highly variable in space and time, involving a “continuous reshuffling of magnetic flux on a time scale of less than 1 minute”. Much of the variability is caused by supersonic flows and shocks, which compress the magnetic fields, especially near the  $\beta = 1$  surfaces.

Further theoretical support may be found in magneto-acoustic shocks which may de-

---

<sup>2</sup>Again we draw on the simulations to examine only the nature of the dynamics of the convectively driven magnetic field in the overlying atmosphere and avoid drawing on properties strongly coupled to the energy equation.

velop preferentially in the cores of the magnetic network, because there the magnetic field expansion is relatively weak. Field-aligned slow mode amplitudes can therefore grow faster in the cores than elsewhere, and will shock lower in the core of the stratified flux tube atmosphere. Indeed Fawzy *et al.* (1998) found the tube expansion profiles to be of critical importance for longitudinal shock-wave heating, and Khomenko *et al.* (2008) found different properties in longitudinal non-linear wave propagation as a function of axial distance in two-dimensional flux-tube models.

In essence, this proposal allows the chromosphere to radiate more without an accompanying increase in the gas pressure and energy density, something which cannot be achieved in static models. We have loosened the (overly-?) restrictive link between radiative energy flux and gas pressure and energy density.

### 3.7.5. *Emission from between flux tubes?*

High resolution data show that photospheric magnetic fields under network boundaries are collections of granular driven field concentrations which, when observed at lower angular resolution, become organized into the familiar chromospheric network. The possibility arises that the “network boundary chromosphere” is then filled with the upward extension of this intermittent field, with a mixture of field strengths and directions which become more uniform with increasing height. It is possible that the UV emission from the network arises predominantly from material *between* these magnetic flux sheets. In this way the pressures of strongly radiating material will be larger than the material embedded within the flux tubes (B.C. Low, private communication 2007). If this proves to be the case, the chromospheric magnetic polarization signatures should be detectably smaller than photospheric extrapolations would indicate. Magnetic signatures are present in chromospheric lines so that not all of the emission can be from field-free plasma (Giovanelli 1980; Pietarila *et al.* 2007a), but such a quantitative comparison remains to be done. Note that such a picture does not discount magnetic heating mechanisms, because the kinetic energy in, e.g., transverse wave motions of the flux tubes will move field-free neighboring fluid, leading perhaps to dissipative compressive waves, for example.

## 4. Conclusions and further speculations

Natural explanations for the local confinement of the bright photospheric and transition region plasmas to the network boundaries have existed for many years. However, we have



identified a possible problem in trying to explain why the chromospheric network emission should also be confined locally, assuming, as seems unavoidable, that increased brightness is associated with increased dissipation of mechanical energy and hence increased temperatures and pressures. Vertical forces may not be sufficient to compress the chromospheric network plasma sufficiently to account for the intense radiation originating there, while at the same time maintaining horizontal pressure balance. The atmosphere has time to equilibrate pressures from the network boundary to the cell interiors (several tens of minutes) compared with the life time of the supergranular structures (30 hours or so), so it is not obvious that magnetostatic equilibrium is a poor approximation on supergranular scales.

Radiation-MHD calculations should ultimately resolve the conundrum posed, firmly constrained by simultaneous spectropolarimetry of the photosphere/chromosphere. Such observations will help clarify issues such as the plasma- $\beta$  state, if field twist is important, or if bright network chromospheric emission arises almost entirely from material preferentially *between* regions of strong field. We can speculate that the resolution of the problem may also provide natural explanations of the time-dependent network boundary chromosphere and spicules. If the network heating is intermittent, then matter will be temporarily over-pressured and will be forced vertically along field lines and expand the field horizontally. Should the pinch effect be important, its non-linear development may explain both chromospheric heating and the ejection of spicules, some of which have significant twisting motions as seen in Hinode (Suematsu *et al.* 2008) and later data (Wedemeyer-Böhm and Rouppe van der Voort 2009). The system may be self-limiting in that more pinch implies more confinement and adiabatic heating, which leads to higher pressures and less confinement (spicule emission?), and so on. This picture is reminiscent of, but different to, the proposition by Athay (2000, 2002) that an ionization instability, caused by the preferential heating of ions in the upper chromosphere, amplifies variable heating rates which in turn lead to the waxing and waning of spicules. The dynamics we envisage might also be related to that seen in 1.5D numerical simulations of randomly driven Alfvén waves in flux tubes by Kudoh and Shibata (1999).

It may be that some Ca II emission is simply re-radiated “hot-wall” radiation from the photosphere. It would be interesting to see 2D radiative equilibrium calculations of flux tube atmospheres instead of semi-empirical thermal structure. This point deserves attention since it is unclear how much of what is traditionally attributed to in-situ chromospheric heating, could instead be simply re-radiated photospheric radiation.

Whatever the outcome, we hope that this discussion will lead to a better understanding of the essential ingredients of the physics of the magnetic network chromosphere, a long standing unsolved problem. It represents by far the biggest “heating problem” in solar physics, needing at least an order of magnitude more energy to sustain it than the overlying

corona.

PJ thanks Yuhong Fan, Boon Chye Low, Mattias Rempel and Han Uitenbroek for many interesting discussions. The VTT is operated by the Kiepenheuer Institut für Sonnenphysik at the Spanish Observatorio del Teide of the Instituto de Astrofísica de Canarias. IBIS was constructed by INAF/OAA with contributions from the University of Florence, the University of Rome, MIUR, and MAE, and is operated with support of the National Solar Observatory. The NSO is operated by the Association of Universities for Research in Astronomy, Inc., under cooperative agreement with the National Science Foundation. We are indebted to DST observers Mike Bradford, Joe Elrod and Doug Gilliam. We thank the anonymous referee for very useful comments.

## REFERENCES

- Alfvén, H.: 1943, *Arkiv for Astronomi* **29A(11)**, 1
- Anderson, L. S. and Athay, R. G.: 1989, *Astrophys. J.* **336**, 1089
- Antiochos, S. K. and Noci, G.: 1986, *Astrophys. J.* **301**, 440
- Athay, R. G.: 2000, *Solar Phys.* **197**, 31
- Athay, R. G.: 2002, *Astrophys. J.* **565**, 630
- Avrett, E. H.: 1981, in R. M. Bonnet and A. K. Dupree (Eds.), *Solar Phenomena in Stars and Stellar Systems*, Reidel: Dordrecht, 173
- Beckers, J. M.: 1972, *Ann. Rev. Astron. Astrophys.* **10**, 73
- Bello González, N. and Kneer, F.: 2008, *Astron. Astrophys.* **480**, 265
- Berger, T. E., Rouppe van der Voort, L. H. M., Löfdahl, M. G., Carlsson, M., Fossum, A., Hansteen, V. H., Marthinussen, E., Title, A., and Scharmer, G.: 2004, *Astron. Astrophys.* **428**, 613
- Bruls, J. H. M. J. and Von der Lühe, O.: 2001, *Astron. Astrophys.* **366**, 281
- Cally, P. S. and Robb, T. D.: 1991, *Astrophys. J.* **372**, 329
- Carlsson, M. and Stein, R. F.: 1995, *Astrophys. J.* **440**, L29
- Carlsson, M. and Stein, R. F.: 1997, *Astrophys. J.* **481**, 500

- Cavallini, F.: 2006, *Solar Phys.* **236**, 415
- Cowling, T. G.: 1976, *Magnetohydrodynamics*, Monographs on Astronomical Subjects, Bristol: Adam Hilger
- de Pontieu, B., McIntosh, S., Hansteen, V. H., Carlsson, M., Schrijver, C. J., Tarbell, T. D., Title, A. M., Shine, R. A., Suematsu, Y., Tsuneta, S., Katsukawa, Y., Ichimoto, K., Shimizu, T., and Nagata, S.: 2007, *Publ. Astron. Soc. Japan* **59**, 655
- Doschek, G. A., Feldman, U., Laming, J. M., Warren, H. P., Schüle, U., and Wilhelm, K.: 1998, *Astrophys. J.* **507**, 991
- Dowdy, J. F., J., Rabin, D., and Moore, R. L.: 1986, *Solar Phys.* **105**, 35
- Fawzy, D. E., Ulmschneider, P., and Cuntz, M.: 1998, *Astron. Astrophys.* **336**, 1029
- Feldman, U.: 1983, *Astrophys. J.* **275**, 367
- Gabriel, A.: 1976, *Phil Trans. Royal Soc. Lond.* **281**, 339
- Giovanelli, R. G.: 1980, *Solar Phys.* **68**, 49
- Giovanelli, R. G.: 1982, *Solar Phys.* **80**, 21
- Hale, G. E. and Ellerman, F.: 1904, *Astrophys. J.* **19**, 41
- Hasan, S. S. and van Ballegoijen, A. A.: 2008, *Astrophys. J.* **680**, 1542
- Judge, P.: 2006, in J. Leibacher, R. F. Stein, and H. Uitenbroek (Eds.), *Solar MHD Theory and Observations: A High Spatial Resolution Perspective*, Vol. 354 of *Astronomical Society of the Pacific Conference Series*, 259
- Judge, P. G. and Carlsson, M.: 2010, *Astrophys. J.* in press
- Judge, P. G. and Centeno, R.: 2008, *Astrophys. J.* **687**, 1388
- Judge, P. G., Tritschler, A., Uitenbroek, H., Cauzzi, G., and Reardon, K.: 2010, *Astrophys. J.* **710**, 1486
- Khomenko, E., Collados, M., and Felipe, T.: 2008, *Solar Phys.* **251**, 589
- Kudoh, T. and Shibata, K.: 1999, *Astrophys. J.* **514**, 493
- Leenaarts, J., Carlsson, M., Hansteen, V., and Rouppe van der Voort, L.: 2009, *Astrophys. J. Lett.* **694**, L128

- Lites, B., Socas-Navarro, H., Berger, T., Frank, Z., Shine, R., Tarbell, T., A., T., Ichimoto, K., Katsukawa, Y., Tsuneta, S., Suematsu, S., Kubo, M., Shimizu, T., and Nagata, S.: 2007, *Astrophys. J.* in press
- Lites, B. W., Rutten, R. J., and Kalkofen, W.: 1993, *ApJ* **414**, 345
- Lites, B. W., Scharmer, G. B., Berger, T. E., and Title, A. M.: 2004, *Solar Phys.* **221**, 65
- Maltby, P.: 1977, *Solar Phys.* **55**, 335
- Mariska, J. T.: 1992, *The Solar Transition Region*, Cambridge Univ. Press, Cambridge UK
- Metcalf, T. R., Jiao, L., McClymont, A. N., Canfield, R. C., and Uitenbroek, H.: 1995, *Astrophys. J.* **439**, 474
- Osterbrock, D. E.: 1961, *Astrophys. J.* **134**, 347
- Parker, E. N.: 1974, *Astrophys. J.* **191**, 245
- Parker, E. N.: 1977, *Astrophys. J.* **214**, 616
- Pietarila, A., Socas-Navarro, H., and Bogdan, T.: 2007a, *Astrophys. J.* **670**, 885
- Pietarila, A., Socas-Navarro, H., and Bogdan, T.: 2007b, *Astrophys. J.* **663**, 1386
- Rammacher, W., Schmidt, W., and Hammer, R.: 2008, *12th European Solar Physics Meeting, Freiburg, Germany, held September, 8-12, 2008. Online at <http://espm.kis.uni-freiburg.de/>, p.2.40* **12**, 2
- Reardon, K. P., Uitenbroek, H., and Cauzzi, G.: 2009, *Astron. Astrophys.* **500**, 1239
- Reeves, E. M.: 1976, *Solar Phys.* **46**, 53
- Schaffenberger, W., Wedemeyer-Böhm, S., Steiner, O., and Freytag, B.: 2005, in D. E. Innes, A. Lagg, and S. A. Solanki (Eds.), *Chromospheric and Coronal Magnetic Fields*, Vol. 596 of *ESA Special Publication*
- Schaffenberger, W., Wedemeyer-Böhm, S., Steiner, O., and Freytag, B.: 2006, in J. Leibacher, R. F. Stein, & H. Uitenbroek (Ed.), *Solar MHD Theory and Observations: A High Spatial Resolution Perspective*, Vol. 354 of *Astronomical Society of the Pacific Conference Series*, p. 345
- Scharmer, G. B., Narayan, G., Hillberg, T., de la Cruz Rodriguez, J., Löfdahl, M. G., Kiselman, D., Sütterlin, P., van Noort, M., and Lagg, A.: 2008, *Astrophys. J. Lett.* **689**, L69

- Schrijver, C. J., Cote, J., Zwaan, C., and Saar, S. H.: 1989, *Astrophys. J.* **337**, 964
- Simon, G. W. and Leighton, R. B.: 1963, *Astron. J.* **68**, 291
- Simon, G. W. and Leighton, R. B.: 1964, *Astrophys. J.* **140**, 1120
- Skartlien, R.: 2000, *Astrophys. J.* **536**, 465
- Skumanich, A., Smythe, C., and Frazier, E. N.: 1975, *Astrophys. J.* **200**, 747
- Socas-Navarro, H.: 2005, *Astrophys. J.* **631**, L167
- Solanki, S., Steiner, O., and Uitenbroek, H.: 1991, *Astron. Astrophys.* **250**, 220
- Solanki, S. K. and Steiner, O.: 1990, *Astron. Astrophys.* **234**, 519
- Solanki, S. K., Steiner, O., and Uitenbroeck, H.: 1991, *Astron. Astrophys.* **250**, 220
- Steiner, O.: 1990, *Astron. Astrophys.* **231**, 278
- Steiner, O.: 2007, in S. Hasan and D. Banerjee (Eds.), *Kodai School on Solar Physics*, No. 919 in AIP Conf. Proc., p. 74
- Steiner, O., Pneuman, G. W., and Stenflo, J. O.: 1986, *Astron. Astrophys.* **170**, 126
- Suematsu, Y., Ichimoto, K., Katsukawa, Y., Shimizu, T., Okamoto, T., Tsuneta, S., Tarbell, T., and Shine, R. A.: 2008, in S. A. Matthews, J. M. Davis, & L. K. Harra (Ed.), *First Results From Hinode*, Vol. 397 of *Astronomical Society of the Pacific Conference Series*, 27
- Tousey, R.: 1971, *Royal Society of London Philosophical Transactions Series A* **270**, 59
- Vecchio, A., Cauzzi, G., Reardon, K. P., Janssen, K., and Rimmele, T.: 2007, *Astron. Astrophys.* **461**, L1
- Vernazza, J., Avrett, E., and Loeser, R.: 1981, *Astrophys. J. Suppl. Ser.* **45**, 635
- Wedemeyer-Böhm, S. and Rouppe van der Voort, L.: 2009, *Astron. Astrophys.* **507**, L9
- Wedemeyer-Böhm, S., Steiner, O., Bruls, J., and Rammacher, W.: 2007, in P. Heinzel, I. Dorotovič, and R. J. Rutten (Eds.), *The Physics of Chromospheric Plasmas*, Vol. 368 of *Astronomical Society of the Pacific Conference Series*, p. 93

Table 1. Log of Ca II H line observations with the VTT ESG

| Date/time<br>UT          | scan<br>number | pointing      | raster<br>parameters    | seeing<br>$r_0$ cm |
|--------------------------|----------------|---------------|-------------------------|--------------------|
| 13 June 2007 10:52-10:56 | 2              | E2.4°, S4.0°  | 241 steps, 1 sec/step   | 7-13               |
| 20 June 2007 8:25-8:31   | 2              | E0.0°, N1.7°  | 240 steps, 1.5 sec/step | 9-12               |
| 20 June 2007 8:39-8:45   | 3              | W19.3°, S6.0° | 240 steps, 1.5 sec/step | 9-13               |

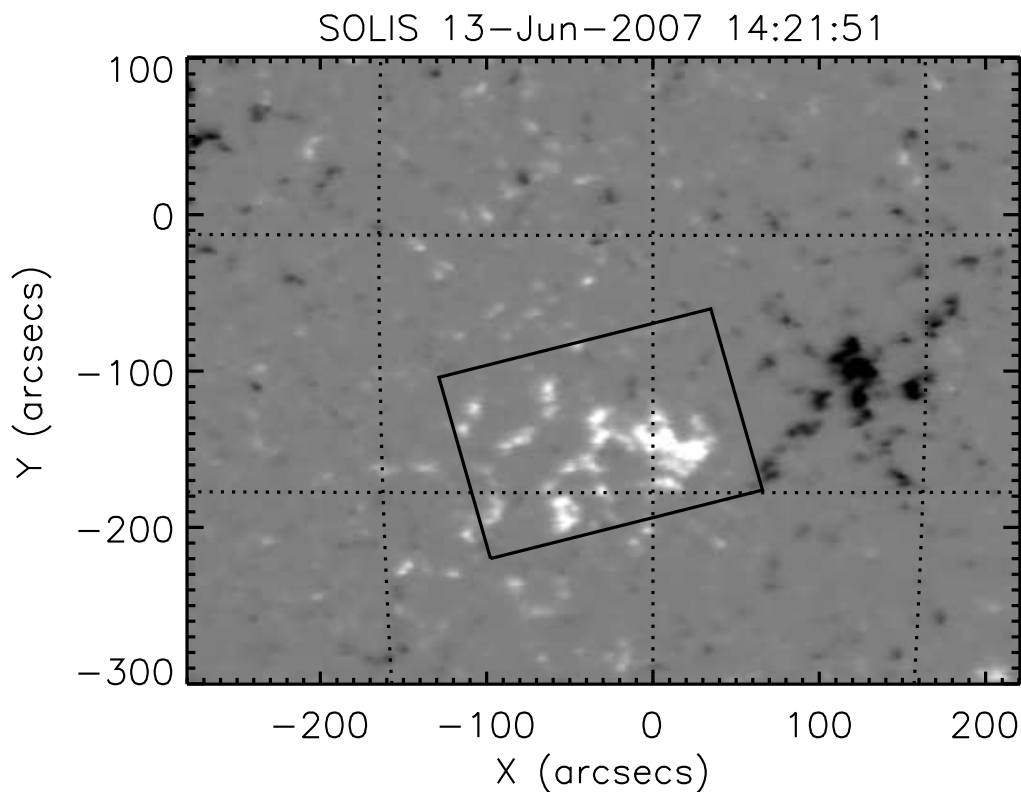


Fig. 1.— A context image of the region observed on June 13 2007 by the ESG. The data show the SOLIS magnetogram obtained at 14:21 UT, rotated back to the epoch of the ESG raster scan (10:52-10:56 UT). The color table is linear between  $\pm 150 \text{ Mx cm}^{-2}$ . The black rectangle indicates the field of view of the Echelle Spectrograph scan.

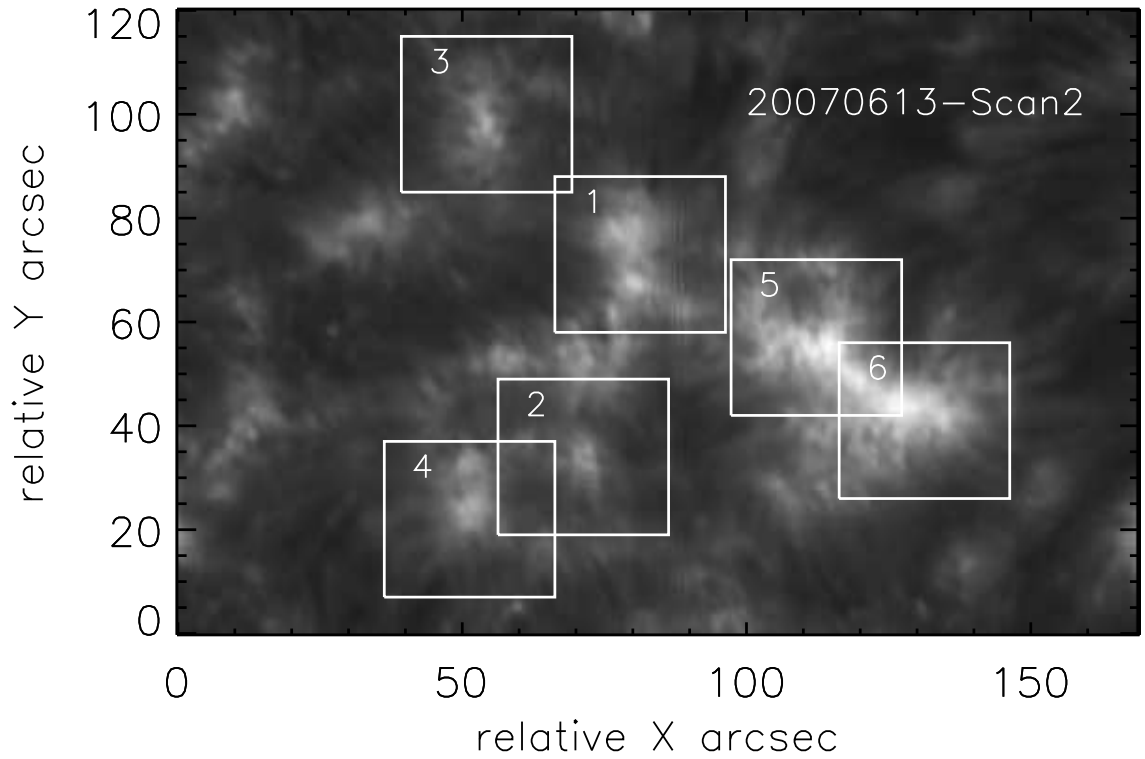


Fig. 2.— The core region of the Ca II H line observed on June 13 2007 by the ESG. The intensities within  $\pm 2.3$  mÅ of the line core are summed and shown in this plot. The boxes labeled 1 through 6 show regions studied in detail in later figures and the text.

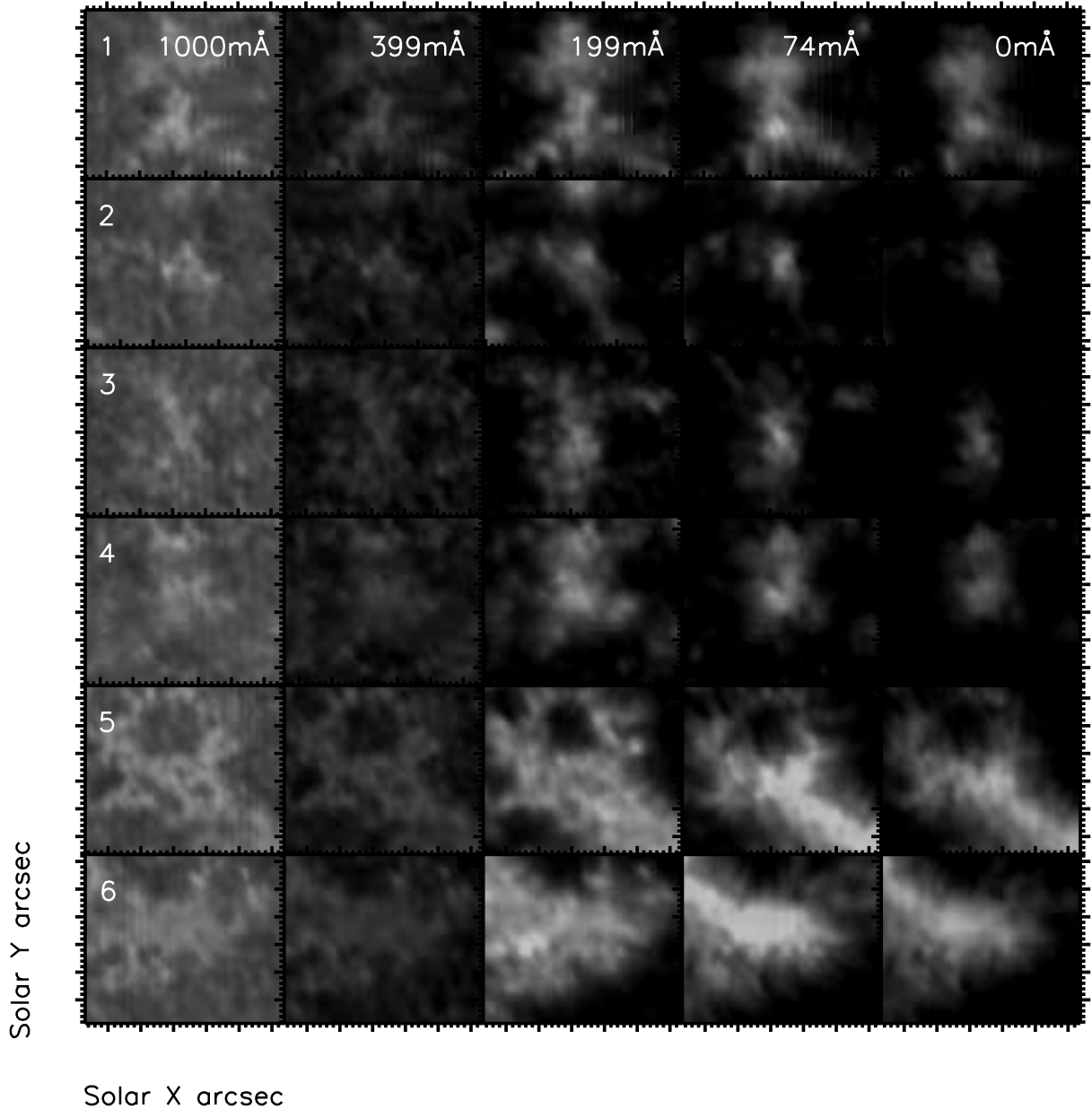


Fig. 3.— “Monochromatic” ESG images, binned over  $22.5 \text{ m}\text{\AA}$  are shown for each boxed region of figure 2, for the data obtained on 13 June 2007. Relative intensities can be compared between all images. Each region is  $30'' \times 30''$  in size, slightly smaller than a typical supergranule cell size. One minor tick mark corresponds to  $1''$ .  $0 \text{ m}\text{\AA}$  corresponds to line center, all other wavelengths are to the red side. The color table is linear, ranges between  $1/4$  and  $1$  of a fixed number of counts, and is the same for all frames.



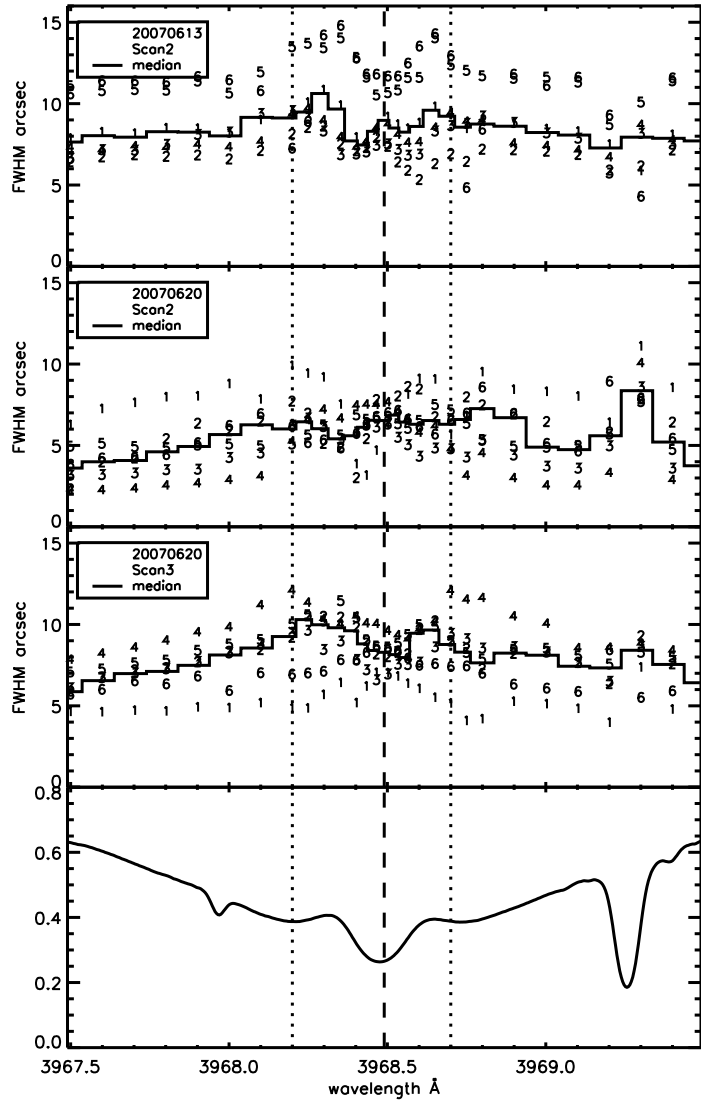


Fig. 4.— Characteristic network widths  $w_N$  plotted as a function of wavelength, for sub-frames of the ESG data shown in Figure 3 and other data (not shown) obtained on 20 June 2007. Solid lines show the median of the autocorrelation widths for the 6 flux concentrations. The numbers correspond to data from the numbered boxes shown in earlier figures. The lowest panel shows the mean spectrum of the data from 13 June 2007, where the data are normalized to the wing intensity near 3966.2 Å. Vertical lines mark locations of the  $H_1$  and  $H_3$  minima.

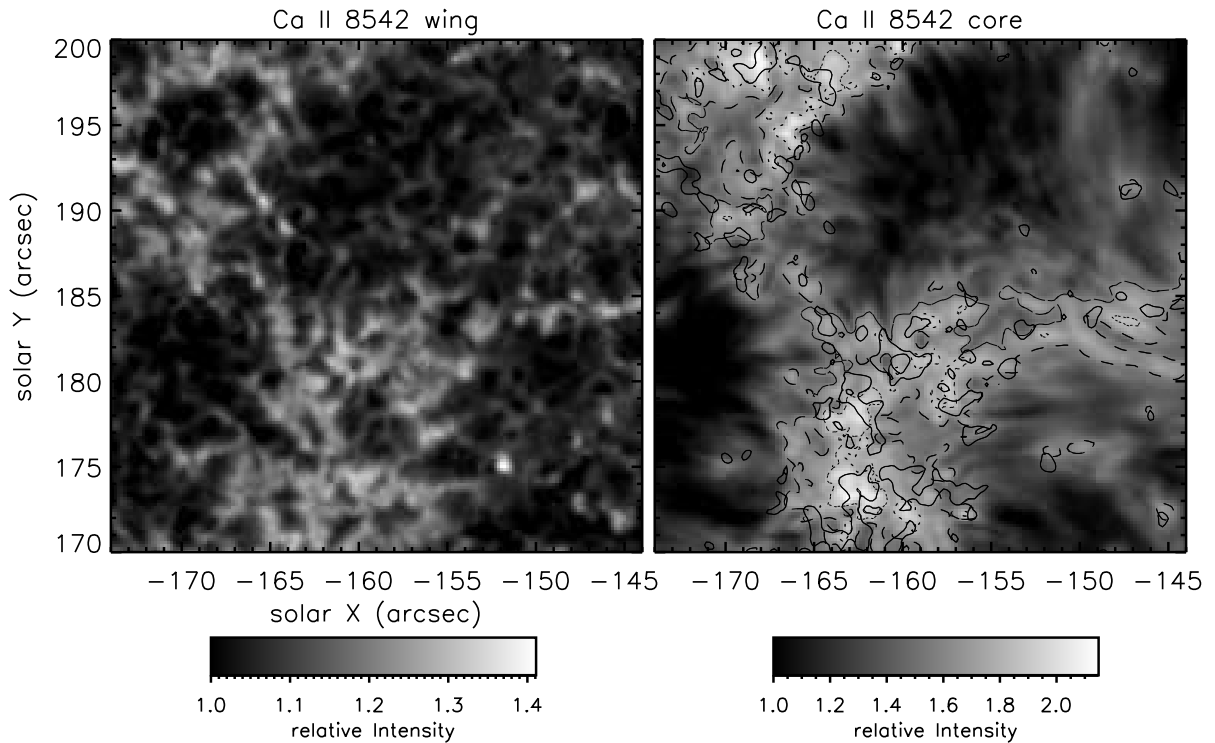


Fig. 5.— Wing (left) and core (right) images of Ca II 8542 Å data obtained 20 May 2008 by Judge *et al.* (2010), using IBIS. The color tables vary from the lowest 5% of the intensity (to remove pixels from the darkest non-magnetic features) to the maximum intensity in each image. The 50% contour of the wing intensity (relative wing intensity of 1.25) is over plotted in the core image (solid lines). The 50% core intensity contour is shown as dashed lines, and the 70% contour of the core image is shown as dotted lines. The 50% core contours are much broader than the 50% wing contours, but the 70% have similar areas. Thus the brightest third or so of the core emission is on small scales similar to those of the wing image (see  $X = -164, Y = 173$ , or  $X = -167, Y = 195$ , for example).

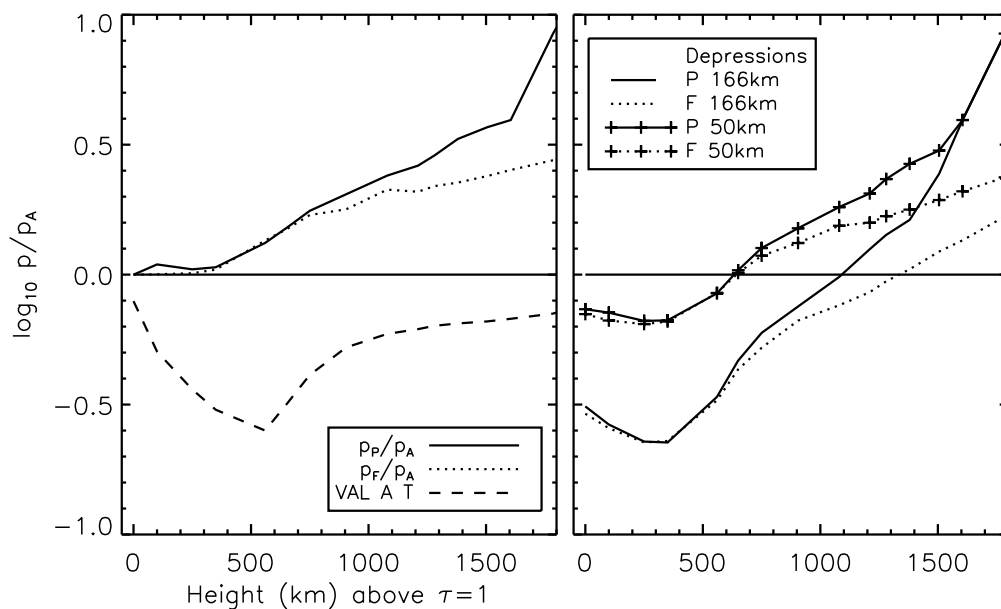


Fig. 6.— Pressure as a function of height in two “flux tube” semi-empirical chromospheric models (models VAL F and P) are plotted, relative to VAL model A. In the left panel, the photosphere is assumed to be at the same physical height in each model. The form of temperature as a function of height for model “A” is shown as a dashed line in the lower half. In the right panel, the “tube” atmospheres, models “F” and “P”, have been shifted downwards by 175 and 90 km.